Development 133, 1911-1921 (2006) doi:10.1242/dev.02363

C. elegans dystroglycan DGN-1 functions in epithelia and neurons, but not muscle, and independently of dystrophin

Robert P. Johnson, Seong Hoon Kang and James M. Kramer*

The *C. elegans* dystroglycan (DG) homolog DGN-1 is expressed in epithelia and neurons, and localizes to basement membrane (BM) surfaces. Unlike vertebrate DG, DGN-1 is not expressed in muscle or required for muscle function. *dgn-1* null mutants are viable but sterile owing to severe disorganization of the somatic gonad epithelium, and show defects in vulval and excretory cell epithelia and in motoneuron axon guidance. The defects resemble those of *epi-1* laminin αB mutants, suggesting that DGN-1 serves as a receptor for laminin. *dgn-1(0)*/+ animals are fertile but show gonad migration defects in addition to the defects seen in homozygotes, indicating that DGN-1 function is dosage sensitive. Phenotypic analyses show that DGN-1 and dystrophin-associated protein complex (DAPC) components have distinct and independent functions, in contrast to the situation in vertebrate muscle. The DAPC-independent functions of DGN-1 in epithelia and neurons suggest that vertebrate DG may also act independently of dystrophin/utrophin in non-muscle tissues.

KEY WORDS: Dystroglycan, Laminin, Dystrophin, Basement membrane, Extracellular matrix, Epithelia, Neurons

INTRODUCTION

Dystroglycan (DG) is a crucial receptor for the basement membrane (BM) in vertebrate muscle. It is composed of an extracellular α subunit and a transmembrane β subunit produced by proteolytic processing of a single precursor (Ibraghimov-Beskrovnaya et al., 1992). Laminin G-like domains in extracellular matrix (ECM) proteins, such as laminin, agrin and perlecan, and the neural cell surface neurexins bind O-linked glycans on α-DG (Hohenester et al., 1999; Michele et al., 2002). β-DG binds to α-DG (Sciandra et al., 2001) and mediates its transmembrane linkage to intracellular cytoskeletal and signaling proteins (Winder, 2001). DG is a component of the skeletal muscle dystrophin-glycoprotein complex (DGC) that includes the transmembrane sarcoglycan complex and the cytoplasmic dystrophin-associated protein complex (DAPC), which contains the actin-binding protein dystrophin, dystrobrevin and syntrophin (Cohn and Campbell, 2000; Winder, 2001). Loss-of-function mutations in DG and other DGC components result in sarcolemmal damage and muscular dystrophy (Cote et al., 1999; Cohn and Campbell, 2000; Cohn et al., 2002; Michele and Campbell, 2003; Parsons et al., 2002).

DG also functions as a BM receptor in non-muscle tissues. Unconditional knockout of DG in mice results in early embryonic lethality due to failure of extraembryonic BM formation (Williamson et al., 1997). DG functions as an important laminin receptor in developing kidney, lung and salivary epithelia (Durbeej et al., 1995; Durbeej et al., 2001). The loss of DG in epithelial-derived breast tumor cells leads to a failure of ECM-induced cell polarization and enhanced invasiveness (Muschler et al., 2002). Brain-specific knockout of DG results in pial BM discontinuities and cortical neuron migration defects (Michele and Campbell, 2003; Moore et al., 2002). Knockout of DG in Schwann cells produces defects in myelination and nodal architecture (Saito et al., 2003). The importance of DGC components to DG function outside of muscle is unclear, as mice lacking both dystrophin and utrophin, or the sarcoglycan complex, do not display the nervous system defects or embryonic lethality seen in the brain-specific and unconditional DG knockouts, respectively (Rafael et al., 1999; Imamura et al., 2000).

Homologs of DG and other DGC components have been identified in *Drosophila melanogaster* and *Caenorhabditis elegans* (Dekkers et al., 2004; Deng et al., 2003; Grisoni et al., 2002). *Drosophila* DG is expressed in follicle and imaginal disc epithelia and the oocyte, and its loss disrupts epithelial and oocyte polarity (Deng et al., 2003). *Drosophila* DG and other DGC components are also expressed in the nervous system and some muscle (Dekkers et al., 2004). In *C. elegans*, DAPC complex homologs function in muscle with the acetylcholine transporter SNF-6 to regulate cholinergic stimulation (Bessou et al., 1998; Gieseler et al., 2001; Grisoni et al., 2003; Kim et al., 2004), but the roles of other DGC components have not been extensively characterized.

We report the characterization of DGN-1, the *C. elegans* ortholog of vertebrate DG. DGN-1 is expressed in epithelia in the gonad and other tissues, and in neurons. DGN-1 is not found in muscle and does not function with the conserved DAPC complex in *C. elegans* muscle. DGN-1 plays an important role in gonad epithelial development, where it is likely to mediate the function of laminin. DGN-1 also affects guidance and the extension of cell processes along BM surfaces. These findings suggest a conserved role for DG in mediating epithelial and neural cell responses to the ECM.

MATERIALS AND METHODS

Culture techniques

Culture and manipulation of *C. elegans* were performed according to standard methods (Brenner, 1974) at 20°C. The following strains were used: wild-type N2 var. Bristol; NJ52 *epi-1(rh27)*; NJ244 *epi-1(rh92)*; NJ590 *epi-1(rh199)*; LS292 *dys-1(cx18)*; LS505 *dyb-1(cx36)*; LS721 *stn-1(ok292)*. The following GFP markers were used: DA/DB motoneurons, *evIs82* [*unc-129*::GFP]; early somatic gonad cells/distal tip cell, *qIs19* or *qIs56* [*lag-2*::GFP]; spermatheca, *jcIs1* [AJM-1::GFP]; gonad sheath, *tnIs6* [*lim-7*::GFP]; anchor cell and body wall muscle, *syIs49* [*zmp-1*::GFP]; *mIs11* [*myo-2*::GFP, *pes-10*::GFP, gut promoter::GFP], chromosome III integrant; *qIs54* [*myo-2*::GFP, *pes-10*::GFP, gut promoter::GFP], X chromosome integrant; *oxIs12* [*unc-47*::GFP], X chromosome integrant. *dgn-1(cg121)*

Department of Cell and Molecular Biology, Feinberg School of Medicine, Northwestern University, Chicago, IL 60611, USA.

*Author for correspondence (e-mail: jkramer@northwestern.edu)

Accepted 15 March 2006

was maintained as a heterozygote balanced by visible X chromosome markers. Alleles of *epi-1* were balanced by *mIs11*. Extrachromosomal arrays of *dgn-1* promoter reporter or GFP fusion protein constructs were created by germline injection (Mello et al., 1991). The laminin-β GFP fusion, *urEx131* [LAM-1::GFP], and EPI-1 antibody were generous gifts of Bill Wadsworth (Robert Wood Johnson Medical School).

dgn-1 genomic and cDNA constructs

The *C. elegans* DG homolog (T21B6.2) was identified by BLAST searches and designated *dgn*-1. Sequencing of the yk671e7 cDNA extended the predicted 5′ end of exon 1 to nucleotide 10315 of cosmid T21B6 (GenBank Z68011), and the 3′UTR to nucleotide 1837. A genomic *dgn-1* clone (pJK600) was constructed by inserting 1181-12990 of T21B6 into the *Xba*I site of BlueScribe M13 Plus (Stratagene). This region includes 2680 bp upstream of exon 1 through the entire 3′UTR of *dgn-1*. pJK600-containing transgenes rescue *dgn-1(cg121)* phenotypes, with ~90% of transgenic animals having restored fertility.

dgn-1::GFP

Plasmid pJK602 contains 2680 bp upstream of exon 1 through the middle of exon 2 (4679-12990 of T21B6) inserted between the *Mlu*I and *Hin*dIII sites of pJJ471. The GFP fusion product contains the first 54 amino acids of DGN-1, a synthetic transmembrane region and GFP. An identical expression pattern was observed with a similar reporter containing only 213 bp upstream of exon 1, suggesting that the major *dgn-1* expression controls are in intron 1.

DGN-1::GFP

Plasmid pJJ516 was made by inserting GFP from pPD114.38 (www.ciwemb.edu/pages/resources.html) into the *Hin*dIII site near the end of the *dgn-1* coding sequence. The product contains GFP inserted after residue 575 of DGN-1, with the final seven DGN-1 residues at the C terminus. Expression of DGN-1::GFP is identical to that of the *dgn-1*::GFP promoter reporter, and DGN-1::GFP rescues the sterility of *dgn-1(cg121)*.

Bacterially expressed DGN-1 fusions

DGN-1 regions corresponding to vertebrate α-DG (amino acids 20-379;TRVF…NSFT) and β-DG (amino acids 392-584;VAFS…FIPP) were PCR amplified from yk671e7 and cloned into pGEX-4T1 (Pharmacia) and pMal-c2 (New England Biolabs) to produce glutathione S-transferase (GST) and maltose binding protein (MBP) fusions. Primers used were:

DGN-1α forward, 5′-CCGCTCGAGACCCGTGTGTTTATTGG-3′;

DGN-1α reverse, 5′-GGCCTCGAGCTAAGTGAAACTGTTGACTGG-3′;

DGN-1β forward, 5′-CCGCTCGAGGTGGCTTTCAGCAACAAT-3′; and

DGN-1β reverse, 5′-GGCCTCGAGTTAAGGAGGAATGAATGG-3′.

GST-DGN-1 fusion proteins were used as immunogens for the production of rabbit and chicken antibodies, which were affinity purified on MBP-DGN-1 columns.

Deletion mutagenesis

Deletion mutagenesis was performed essentially as described (Barstead, 1999). Progeny of trimethylpsoralen/UV mutagenized animals were screened by PCR for deletions in *dgn-1*. The *cg121* deletion removes nucleotides 2045-4439 of cosmid T21B6. The *cg121* mutant strain was backcrossed to wild type at least six times before further analyses.

Western blot analysis

Embryos and mixed larval stage animals were pulverized in liquid nitrogen and extracted in PBS, 1% NP40 containing protease inhibitor cocktail (Roche Biochemical). Extracts were centrifuged (50,000 ***g***, 20 minutes, 4°C) to remove insoluble material. Alternatively, 25 adults were boiled for 15 minutes in 2% SDS containing protease inhibitors and centrifuged (14,000 ***g***, 10 minutes, 4°C). Extracts were subjected to SDS-PAGE and transferred to nitrocellulose. Filters were blocked in PBS containing 5% non-fat dried milk, incubated with affinity-purified anti-DGN-1 antibody followed by horseradish peroxidase-conjugated secondary antibody (Vector Laboratories), and developed for ECL chemiluminescent detection (Amersham Pharmacia Biotechnology).

For deglycosylation experiments, extracts were adjusted to 1% SDS and boiled for 10 minutes. After cooling, nine volumes of 0.5% NP40, 50 mM Tris-HCl (pH 8.0) containing protease inhibitors was added and samples were digested for 16 hours at 37°C with 1 unit of protein-N-glycosidase F (PNGaseF; New England Biolabs).

Microscopy

Animals were mounted on thin pads of 2% agarose in a drop of M9 buffer (Wood, 1988) containing levamisole (0.1 mM) or sodium azide (10 mM) to immobilize them. Immunohistochemistry was performed as described (Kang and Kramer, 2000). Monoclonal anti-MHC-A myosin, polyclonal anti-LET-2, polyclonal anti-NID-1, and polyclonal anti-EPI-1 antibodies were used as described (Kang and Kramer, 2000; Huang et al., 2003). Polyclonal anti-DGN-1 was used at a 1:100 dilution. Images were collected on a Zeiss Axiophot microscope equipped with a CCD camera. Some fluorescent images were deconvolved (VayTek MicroTome) to remove out-of-focus signals.

Expression of differentiated gonad cell markers in *dgn-1(0)*

Assessment of L4 or adult stage *dgn-1(0)* animals using integrated GFP markers and/or morphology revealed that: 98% have one to two distal tip cells (strong *qIs56*[*lag-2*::GFP]); 99% have one to two clusters of presumptive spermathecal cells (strong *jcIs1*[*ajm-1*::GFP]); 90% form one to two anchor cells (*syIs50*[*zmp-1*::GFP]); 89% have presumptive gonad sheath cells (*tnIs6*[*lim-7*::GFP]); and 63% show a peri-vulval lumen in mid/late L4 stage, indicative of uterine tissue (*n*=95-100 animals scored for each marker).

Behavioral assays

For activity on plates, individual L4 stage animals were transferred to NGM plates without bacteria and allowed to recover for 1 minute before counting the number of body bends in a 2-minute interval. For thrashing in liquid, L4 animals were transferred to a drop of M9 medium on an unseeded NGM plate, allowed to recover for 1 minute, then filmed for 2 minutes. The number of body bends, defined as a reversal in direction of head movement, was counted from recordings. For defecation assays, the timing of successive posterior body contraction and expulsion steps (Avery and Thomas, 1997) on seeded NGM plates was recorded for 10 defecation cycles. Assays were performed at room temperature (approximately 22°C).

RESULTS

Three DG-like genes in *C. elegans*

Three *C. elegans* genes encode DG-like proteins, *dgn-1* (T21B6.2), *dgn-2* (F56C3.6) and *dgn-3* (F07G6.1). DGN-1 is the most similar in sequence and structural organization to vertebrate and *Drosophila* DGs (Fig. 1B,C). DGN-1 contains the N-terminal immunoglobulin-like domain of vertebrate α-DG (Bozic et al., 2004), which is missing from *Drosophila* DG (Fig. 1B, N-terminal). A threonine-rich, mucin-like region is present in all DGs, although it is much shorter in DGN-1 (Fig. 1B, N-terminal). *dgn-1* orthologs in the nematodes *C. briggsae* (CBG17551) and *C. remanei* (ORF on Contig1797.2) show strong conservation of sequence (80-90% identity) and domain organization with DGN-1.

Specific functional amino acid residues are conserved in all DGs, including two cysteine pairs that form disulfide bonds in vertebrate DG (Brancaccio et al., 1998; Deyst et al., 1995) and several predicted N-linked glycosylation sites (Fig. 1B). Two regions of sequence divergence are noteworthy. First, neither invertebrate DG shows strong sequence conservation in the vertebrate α/β proteolytic cleavage region (Fig. 1B, core). Second, crucial residues for binding WW and SH3 domain-containing proteins such as dystrophin (Huang et al., 2000) are not conserved in DGN-1 (Fig. 1B, cytoplasmic). These differences are also true for the *C. briggsae* and *C. remanei* orthologs (data not shown).

DGN-2 and DGN-3 share only the DG core with vertebrate DG, corresponding to the α-DG C terminus and the β-DG N terminus (Fig. 1B). In addition to the *dgn-1* ortholog, *C. briggsae*

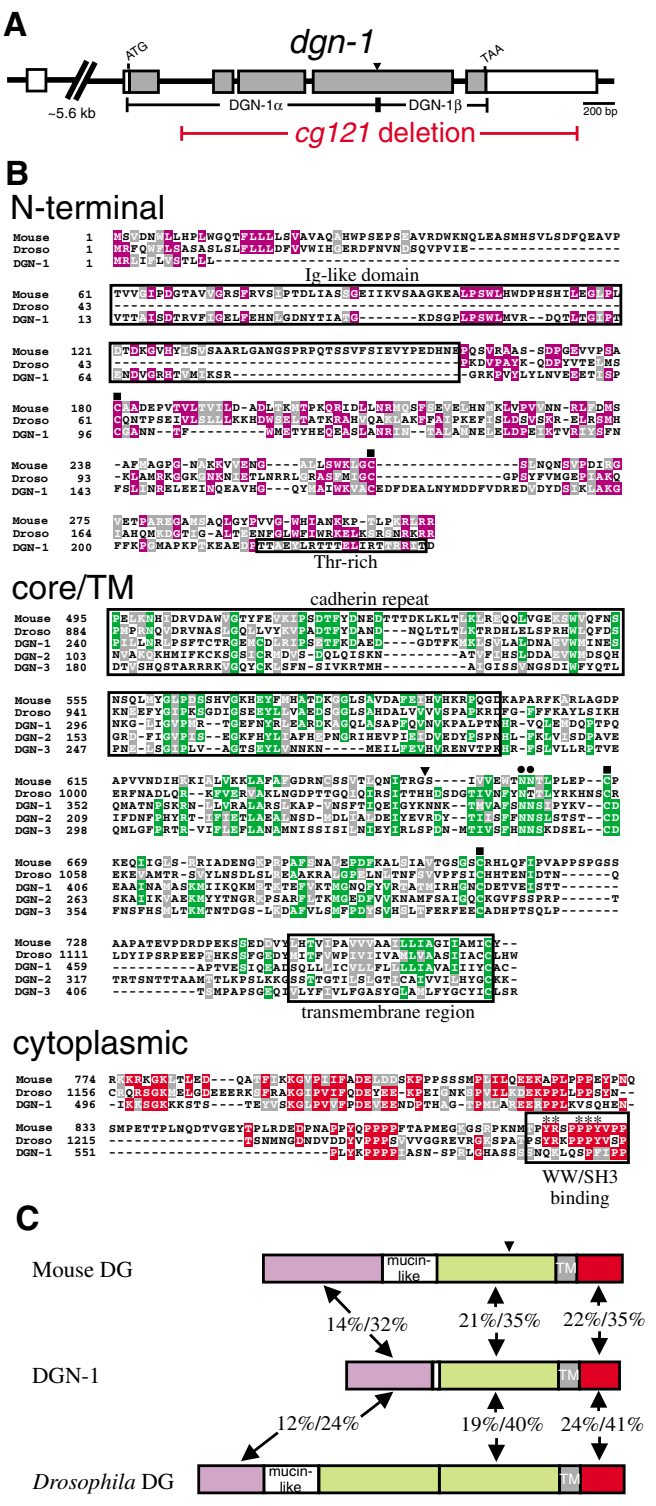

Fig. 1. Structure of the *dgn-1* gene and product. (**A**) Coding (gray) and non-coding (white) exons of *dgn-1*; regions corresponding to α- and β-DG, the site of α/β cleavage in vertebrates (arrowhead), and the extent of the *cg121* deletion are indicated. (**B**) Three regions of similarity to vertebrate (mouse) and *Drosophila* DGs were identified, corresponding to the N-terminal domain of α-DG, the C-terminal region of vertebrate α-DG plus extracellular region of β-DG (core domain), and the β-DG cytoplasmic domain. A transmembrane (TM) region follows the core. Amino acids retained in a majority of the sequences are shown in color (N-terminal, purple; core and transmembrane, green; cytoplasmic, red), similar residues in gray. Two additional predicted DG-like proteins in *C. elegans*, DGN-2 and DGN-3, contain a core domain but lack similarity to DG outside of the core (not shown). Conserved cysteine pairs (■) in N-terminal and core domains, conserved predicted *N*-glycosylation sites (●) in the core domain, and the α/β cleavage sitein vertebrate DG (▼) are indicated. A 20-residue threonine-rich region in the DGN-1 N-terminal domain may function as a mucin-like region. Residues mediating interaction of the β-DG cytoplasmic tail with WW/SH3 proteins such as dystrophin are indicated (asterisks). (**C**) Pairwise sequence similarity (% identity/% similarity) between conserved regions. Regions of similarity were identified by BLAST (Altschul et al., 1990) and sequence alignments constructed using Clustal W (Thompson et al., 1994).

(CBG16240) and *C. remanei* also have other predicted gene products containing a DG core. This region therefore defines a family of DG-like proteins. *Drosophila* DG contains two adjacent, divergent copies of this core region (Sciandra et al., 2001). Outside of the core, DGN-2, DGN-3 and CBG16240 show no similarity to each other or to other DG family members. Thus DGN-1 is the unique nematode ortholog of vertebrate DG, and additional species-specific DG-like proteins with variable N-terminal and cytoplasmic domains have arisen in nematodes.

DGN-1 is a glycoprotein that is not processed into separate α and β subunits

Antibodies against DGN-1 regions corresponding to vertebrate α- or β-DG were used to detect DGN-1 in lysates of embryos and larvae. Both antibodies detected a band of ~85 kDa, higher than the 68 kDa predicted mass (Fig. 2A). No bands corresponding to separate DGN-1α or β species were detected, indicating that DGN-1 is not processed into separate α and β subunits. Embryonic DGN-1 migrates as a compact 85 kDa band and a minor 95 kDa species (Fig. 2C, lane 1), and larval DGN-1 as a heterogeneous band centered around 85 kDa (Fig. 2C, lane 3). PNGase F digestion of embryo extracts shifts the 85 kDa species to a 75 kDa band (Fig. 2C, lane 2). The 95 kDa band shifts slightly to ~90 kDa, suggesting differential N-glycosylation of this species. PNGase F digestion of larval extracts results in widening of the DGN-1 band and a 10-15 kDa decrease in median apparent weight (Fig. 2C, lane 4). Thus, larval DGN-1 is also N-glycosylated, but its heterogeneity is largely determined by other modifications, possibly including O-glycosylation as occurs with vertebrate α-DG.

DGN-1 is expressed in epithelial and neural tissues, but not in muscle

Sites of *dgn-1* expression were determined using reporters driven by *dgn-1* upstream sequences. In early (pre-morphological) embryos, *dgn-1*::GFP expression is evident in many epithelial and neural precursors comprising the outer layer of cells (Fig. 3A). As elongation begins at comma stage, expression becomes most prominent in several specialized epithelial cells, including pharyngeal e2 and marginal cells, excretory cells, the somatic gonad precursors (SGPs) Z1 and Z4, and rectal epithelial cells (Fig. 3B). Weaker expression is apparent in hypodermal precursors and neuroblasts along the ventral midline. Pharyngeal expression persists through the L3 larval stage, whereas excretory and rectal cell expression persists throughout development. SGP expression (Fig. 3C,E) persists in SGP descendants, such as the distal tip cells (DTCs; Fig. 3I), and increases throughout the gonad during the L4 stage (Fig. 3J). Variable, generally weak expression is seen

throughout larval development in several neurons, although PVP neurons show strong expression throughout development (Fig. 3C,F). Transient increased expression occurs in new P cell-derived neurons in the ventral nerve cord in late L1/early L2 stage animals (Fig. 3H). Variable weak expression is seen in hypodermal cells, principally hyp5 in the head (Fig. 3D). Preceding the L4/adult molt, expression increases in the vulval epithelium (Fig. 3K).

The expression pattern was confirmed and subcellular localization determined using anti-DGN-1 antibody staining and analysis of a rescuing DGN-1::GFP fusion protein. Both approaches yielded similar results, which are described for antibody staining. In pre-morphological embryos, DGN-1 is diffuse around the surface of outer ectodermal cells before BMs form (Fig. 4A), but begins to polarize towards basal surfaces as BMs assemble between germ layers (Fig. 4B). Throughout subsequent development, DGN-1 localizes to the basal surfaces of pharyngeal (Fig. 4C), gonadal (Fig. 4C-G), rectal (Fig. 4H), vulval (Fig. 4E,F) and excretory cell (Fig. 4I,K) epithelia, in close apposition to the underlying BM. DGN-1 accumulation is more variable in the hypodermis (Fig. 4K,L) and neurons (Fig. 4J).

DGN-1 antibodies show no detectable staining of muscle, although DGN-1 is present in the epithelium immediately adjacent to muscles (Fig. 4K,L). Staining was not detected in body wall, pharyngeal or specialized muscles of the alimentary and reproductive systems. Moreover, neither the *dgn-1*::GFP promoter reporter nor the rescuing DGN-1::GFP fusion show expression in muscle. Thus, DGN-1 is notably different from vertebrate DG, as a role for DGN-1 in muscle function is unlikely.

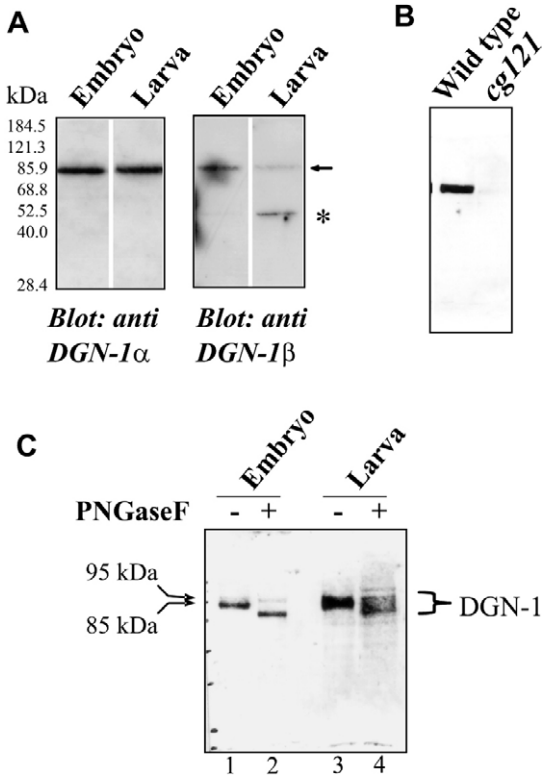

Fig. 2. DGN-1 is glycosylated but not cleaved into α/β subunits. (**A**) Antibodies to DGN-1 regions corresponding to α-DG and β-DG detect a single major band at 85 kDa (arrow) on western blots of embryo or mixed larval extracts. The anti-DGN-1β antibody cross-reacts with a bacterial antigen in the larval extract (asterisk). (**B**) DGN-1 is absent from *dgn-1(cg121)* lysates probed with anti-DGN-1α, demonstrating that *cg121* is a molecular null allele. The extract from 25 adult animals was run in each lane. (**C**) Extracts digested with PNGaseF (protein N-glycosidase F) to remove N-linked glycans (lanes 2,4) were western blotted with anti-DGN-1α antibody. The compact 85 kDa species in embryos shifts to 75 kDa after digestion, near to the predicted polypeptide size. In larval extracts, the broad DGN-1 band decreases in molecular weight after digestion but remains heterogeneous, indicating the presence of N-glycosylation and some additional modification(s), possibly O-glycosylation.

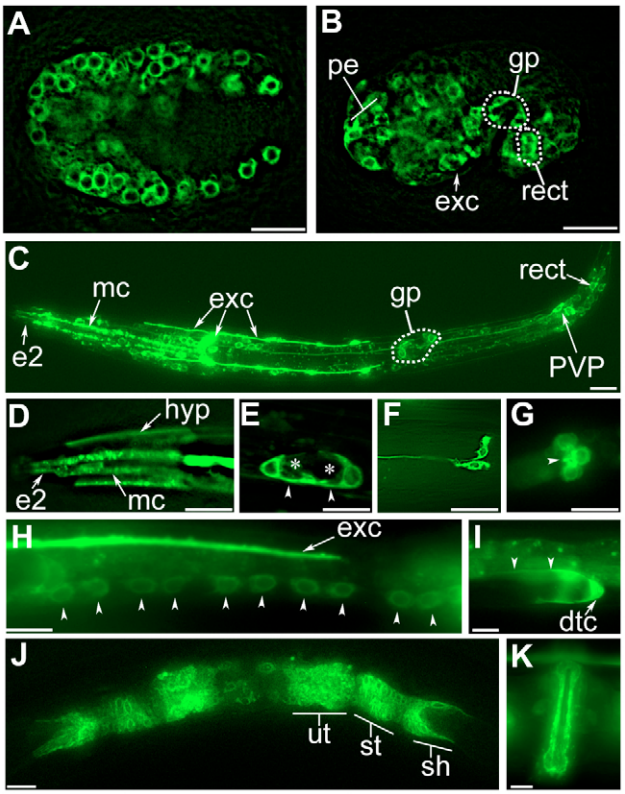

Fig. 3. *dgn-1* is expressed in epithelia and neurons. (**A**) In early embryos, *dgn-1*::GFP is expressed in epithelial and neural precursors in the outer layer of cells. (**B**) As elongation begins, expression becomes prominent in pharyngeal epithelia (pe), the excretory cell (exc), the two somatic gonad precursors in the gonad primordium (gp), and in rectal epithelia (rect). Weaker expression is seen in a number of hypodermal and neural precursors. (**C**) In early larvae, expression persists in the e2 and marginal (mc) cells of the pharyngeal epithelium, the excretory cell, the gonad primordium and the rectal epithelium. Strong expression is seen in the PVP neurons. (**D-G**) Enlarged images showing expression in: (D) the pharyngeal epithelium and hypodermal cell hyp5 (hyp); (E) somatic gonad precursors, which project processes (arrowheads) around the primordial germ cells (asterisks); (F) PVP neurons; (G) rectal epithelial cells, which project processes (arrowhead) around the rectal sphincter. (**H**) Transient expression during late L1 stage in P-cell-derived ventral cord neurons (arrowheads). (**I**) A L3 stage animal showing expression in the distal tip cell and gonad epithelium (arrowheads). (**J**) Strong expression in L4/adult stage gonad, including the uterus (ut), spermatheca (st) and sheath (sh). (**K**) Expression in late L4 stage vulval epithelium. Scale bar: 10 μm.

A dgn-1 null mutant shows defects in epithelial and neural tissues but not in muscle

We isolated a deletion, *cg121*, that removes most of the coding and some of the 3′ untranslated region of *dgn-1*. Western (Fig. 2B) and northern blot (not shown) analyses showed that *cg121* is a molecular null allele. Homozygous *dgn-1(cg121)* animals are viable but sterile (Fig. 5), and display epithelial and neural defects.

Sterility results from an early disruption of gonad morphogenesis. The wild-type gonad primordium contains two central primordial germ cells (PGCs) flanked at anterior and posterior poles by the two SGPs. The primordium is compact, with a sharp DIC image boundary, indicating a robust surrounding BM (Fig. 5C). In newly hatched *cg121* homozygotes, the primordium is usually compact but often displays bulging of PGCs and a weak DIC boundary (Fig. 5D). SGPs are frequently displaced from the poles, sometimes interposing between PGCs (Fig. 5D,H). In some *cg121* larvae, no DIC boundary is detectable and gonadal cells spread dorsally along the body wall (Fig. 5E). Older *dgn-1* mutants often show swelling in the mid-body region as a result of body wall muscle cell fusion with, or engulfment of, loose germ cells (data not shown), as is also seen in *epi-1* laminin mutants (Huang et al., 2003).

The aberrant gonad morphology of *dgn-1* mutants suggests defects in the gonad BM. Antibodies to collagen IV and nidogen, and a LAM-1(laminin-β)::GFP fusion were used to examine the distribution of BM components. In early *cg121* L1 larvae with compact gonad primordia, localization of BM components around the primordium appears normal (Fig. 6). In larvae with disrupted primordia, localization of BM components is still seen, but staining is weak and diffusely distributed over the surface of the gonad tissue (not shown). Thus, a BM organizes around the *dgn-1(0)* gonad but is not maintained. No gross alteration in other BMs is seen in *dgn-1* mutants.

Failure of gonad primordium BM function in *dgn-1* mutants may result from an inability of SGPs to form a stable epithelial layer around the PGCs. Mispositioned SGPs, showing strong association of laminin-β::GFP, can be observed covering one PGC while excluding the other (Fig. 6F,G). Thus, the extrusion of germ cells probably reflects a failure of the somatic gonad epithelium and its associated BM to provide a stable barrier.

Organization of gonad tissue in *dgn-1(0)* animals was examined following the L1/L2 molt, using *lag-2*::GFP expression and nuclear morphology to discriminate somatic and germ cells. Early L2 *dgn-1(0)* animals contained 8.8±1.0 somatic gonad cells (n=25), which is close to the wild-type number of 8. The somatic gonad cells of *dgn-1(0)* animals cluster together in a central clump, or in a contiguous line (sometimes separated into two clusters) along the ventral surface (Fig. 5J,K). In either organization the somatic cells remain in contact, suggesting somatic cell-cell adhesion is retained.

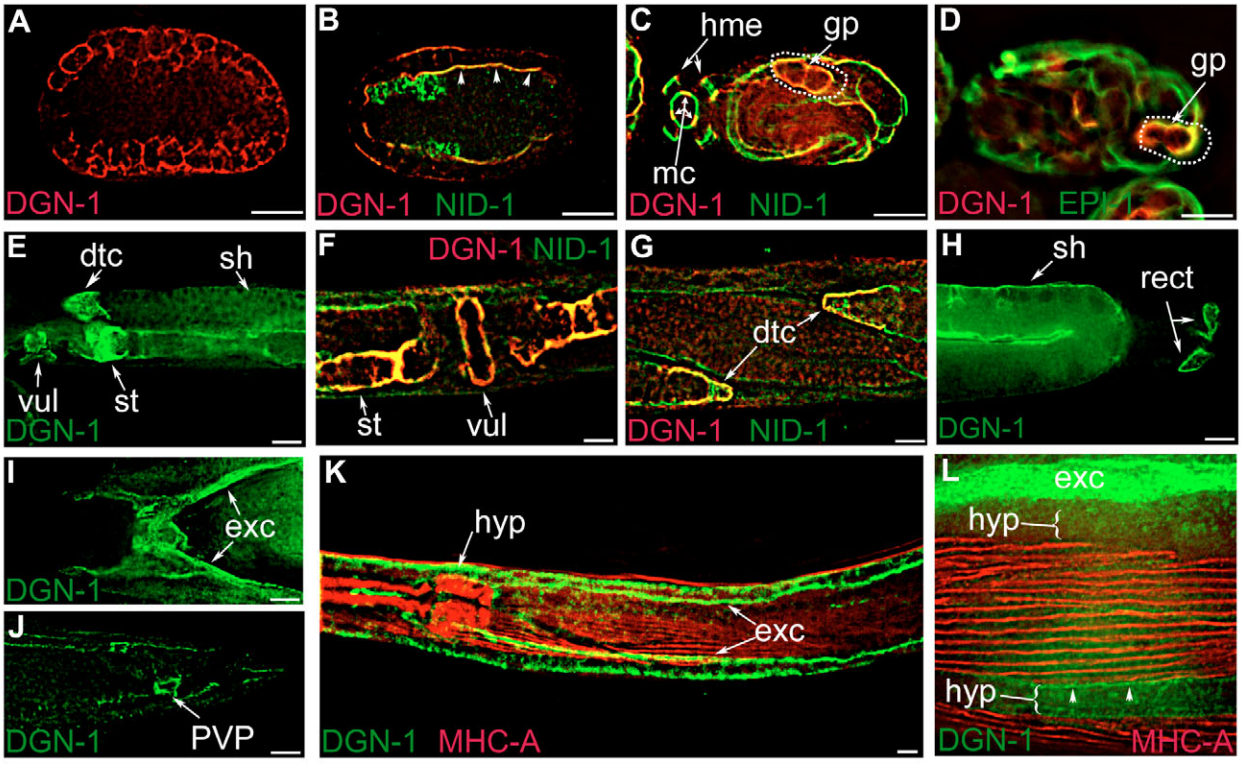

Fig. 4. Localization of DGN-1 in epithelia and neurons, but not muscle. (**A**) In early embryos (pre-lima stage) before BM formation, DGN-1 (red) is distributed around the surface of many epithelial and neural precursors. (**B**) As BMs assemble (lima to comma stages), identified by staining for NID-1/nidogen (green), DGN-1 (red) redistributes to the basal surface (arrowheads). (**C**) In late embryos (pretzel stage), DGN-1 (red) is prominent in marginal cells (mc) and the gonad primordium (gp), and localizes to basal surfaces marked by NID-1 (green). Hypodermal DGN-1 colocalizes with NID-1 at the edges of the body wall muscles (hme). (**D**) DGN-1 (red) and EPI-1/laminin-αB (green) colocalize in the gonad primordium of late embryos (pretzel stage). (**E**) DGN-1 (green) is prominent in spermatheca (st), gonad sheath (sh) and distal tip cells (dtc) of the gonad and the vulval epithelium (vul). (**F**,**G**) In the gonad and vulva, DGN-1 (red) localizes to the BM surface (NID-1, green). (**H**,**I**) DGN-1 (green) is at the basal surface of the rectal epithelium (H, rect) and the excretory cell (I, exc). (**J**) DGN-1 (green) in the PVP neurons. (**K**) DGN-1 (green) localization in the hypodermis (hyp) and excretory cell, but not in body wall or pharyngeal muscle, visualized by staining of MHC-A myosin in muscle M-lines (red). (**L**) DGN-1 (green) is seen weakly throughout the hypodermis covering muscle and is slightly concentrated adjacent to the body wall muscle (arrowheads), but not in the underlying muscle (red). Scale bar: 10 μm.

By contrast, germ cells are either not in contact or only in peripheral contact with somatic cells (Fig. 5J). These results further indicate the inability of somatic cells to associate with or ensheath germ cells in *dgn-1(0)* animals. Monitoring of *dgn-1(0)* gonads throughout the L2 stage did not reveal any overt re-organization of *dgn-1(0)* somatic gonad cells, indicating a failure of somatic primordium formation in *dgn-1(0)* animals. By contrast, wild-type gonads showed reorganization of somatic cells into a central somatic primordium and distal tip cells at the ends of the two emerging gonad arms.

The examination of L4/adult *dgn-1(0)* animals for the expression of markers for differentiated somatic gonad cell types indicated that DTCs, sheath, spermathecal, uterine and anchor cells form in the majority of *dgn-1(0)* animals (see Materials and methods). These results indicate that the expansion and differentiation of somatic gonad cell lineages is not blocked in the absence of DGN-1. Variable expansion of the germ lineage cell population was noted in *dgn-1(0)* animals but the fate of germ cells was not followed

Heterozygous *cg121/+* animals form a grossly normal gonad, but produce 15% fewer progeny than do wild type (wild type, 309±41; *cg121/+*, 263±32; *n*=18). Twenty-three percent of *cg121/+*

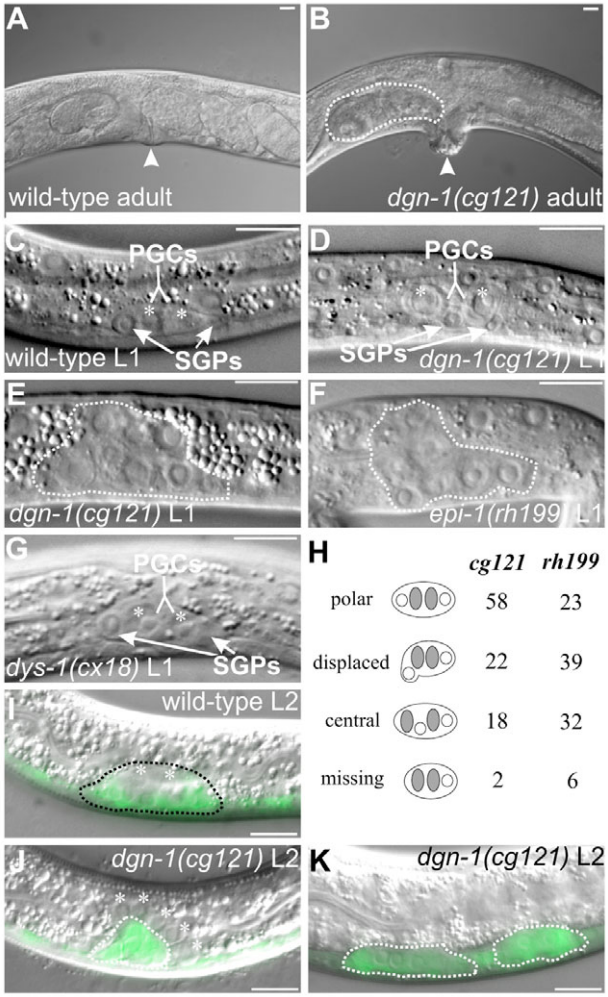

Fig. 5. A *dgn-1* null mutant is viable but sterile due to early gonad disruption. (**A**,**B**). Wild-type (A) and homozygous *dgn-1(cg121)* null mutant (B) adults. Gonad tissue in *cg121* forms a disorganized mass (white outline) and the vulva protrudes (arrowheads). (**C**) Wild-type four-cell gonad primordium with two central PGCs (asterisk) and two SGPs surrounded by a BM creating a sharp DIC boundary. (**D**) Newly-hatched *cg121* homozygotes retain a compact primordium but have mispositioned SGPs, a weak DIC boundary and bulging PGCs. (**E**) Ruptured gonad primordium of a *cg121* L1 larva; gonadal cells spread along the body wall (white outline). (**F**) Early *epi-1(rh199)* laminin αB L1 larva showing similar rupture of the primordium (white outline). (**G**) Normal gonad primordium in *dys-1(cx18)* dystrophin mutant L1 larvae. (**H**) Percentage of mispositioned SGPs in newly-hatched *dgn-1(cg121)* (*n*=104) and *epi-1(rh199)* (*n*=58) larvae. (**I**) Overlay of DIC and *lag-2*::GFP images of wild-type gonad (black outline) at early L2 stage. Somatic gonad cells expressing *lag-2*::GFP (green) are in close association with germ cells (asterisks). (**J**,**K**) DIC/*lag-2*::GFP overlays of gonads in early L2 stage *dgn-1(0)* animals. (J) In 60% (*n*=25) of animals, somatic gonad cells (white outline) form a central cluster separated from, or in only peripheral contact with, germ cells (asterisks). (K) In 40% of animals, somatic gonad cells adopt a contiguous linear arrangement along the ventral surface, sometimes split into two clusters. In I-K, additional *lag-2*::GFP signal from non-gonadal cells is visible along the ventral midline. Scale bar: 10 μm.

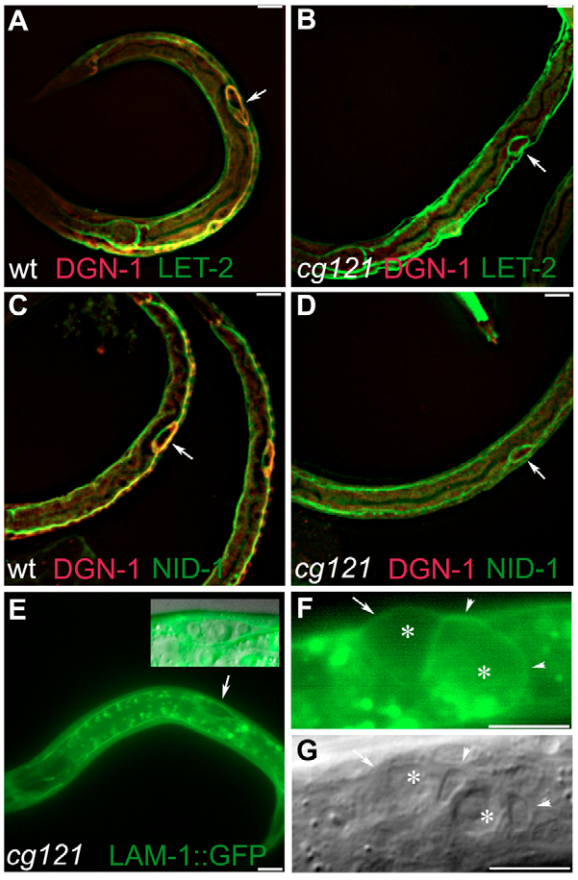

Fig. 6. Localization of BM components to the *dgn-1(0)* gonad. (**A**,**B**) Wild-type (A) and *cg121* homozygote (B) L1 larvae stained with antibodies to collagen α2(IV) LET-2 (green) and to DGN-1 (red). (**C**,**D**) Wild-type (C) and *cg121* homozygote (D) L1 larvae stained with antibodies to nidogen NID-1 (green) and to DGN-1 (red). Early *cg121* larvae retaining a compact gonad primordium show wild-type staining of the gonad primordium with LET-2 and NID-1 antibodies (arrows). (**E**) Early *cg121* homozygote expressing LAM-1::GFP (green); association with the compact gonad primordium is apparent (enlarged with DIC overlay in inset). (**F**) Early *cg121* homozygote with a mispositioned SGP; both SGPs with an associated strong LAM-1::GFP signal (green) ensheath only one (arrowheads) of the two primordial germ cells (asterisks). The unsheathed PGC is only weakly associated with laminin (arrow). (**G**) DIC image of F. Scale bar: 10 μm.

heterozygotes have defects in gonad arm migration (Fig. 7). The arms migrate on the underlying BM led by DTCs, which express DGN-1. Although a range of migration defects is seen in *cg121/+* animals, the occurrence of oblique turns and abnormal midline crossings indicates a failure of DTC responses to BM guidance cues (Su et al., 2000).

Eighty-nine percent of *cg121* animals show defects in formation of the tubular excretory cell arms. Missing or short arms are seen in most *cg121* homozygotes (Fig. 8B,D). Multiple defects can occur in individual animals, but generally only one to two arms are missing or short. Fourteen percent of mutants also have ectopic arms that generally parallel the corresponding normal arm (Fig. 8C,D). Heterozygous *cg121/+* animals show the same range of excretory process defects but at a reduced penetrance (Fig. 8D).

dgn-1 mutants do not have strong movement defects, indicating a severe perturbation of muscle or neural function. However, in 31% of *dgn-1* mutants, at least one DA/DB type neuron commissure extends on the wrong side of the body (Fig. 9A). Individual animals also show additional axonal defects, such as defasciculation or abnormal branching (Fig. 9B-D). Heterozygous *cg121/+* animals show similar DA/DB guidance defects but at a lower penetrance.

The vulval epidermis shows prominent *dgn-1* expression starting when the invaginated epidermis everts and tightens into a slit-shaped opening. Forty-five percent of *dgn-1* adults have a protruding vulva (Pvl) phenotype, suggesting a detachment of the vulval epithelium from the underlying tissue (Fig. 5, Table 1). Frequently, rupture at the protruding vulva leads to the herniation of internal organs, indicating that *dgn-1* function is important in the anchorage of the vulval epidermis.

Ten percent of *dgn-1* mutants have two vulvae, while 12% are vulvaless (n=131), suggesting a defect in specification of the vulva-inducing anchor cell (AC) (Greenwald, 1997). Using the AC marker *zmp-1::*GFP (Inoue et al., 2002), we found 14% of *dgn-1* mutants generate two ACs, while 10% fail to generate an AC (n=95). All wild-type animals produced one AC (n=100). This AC specification defect is likely to result primarily from a disruption of gonad structure in *dgn-1* mutants.

dgn-1 mutants do not show phenotypes associated with defects in muscle function, such as Pat (paralyzed at two-fold) or Unc (uncoordinated movement). No gross disorganization of body wall muscle was apparent by DIC microscopy. The muscles associated with the alimentary system function normally, while function of uterine and vulval muscles cannot be assessed because of the failure of gonad formation in *dgn-1* mutants.

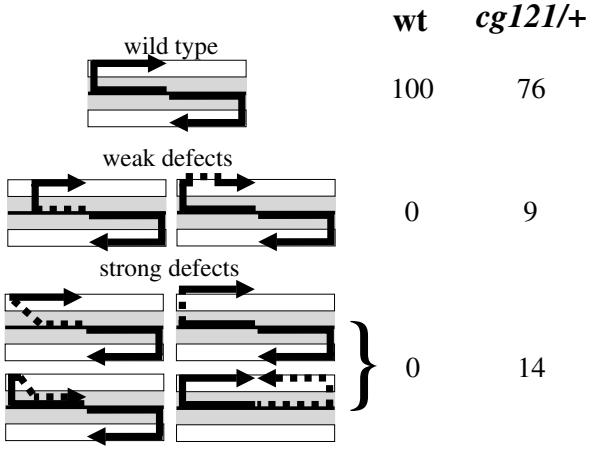

Fig. 7. Gonad migration defects in *cg121* heterozygotes. The percentages of *cg121/+* animals showing the indicated type of DTC migration defects is shown.

dgn-1 phenotypes are similar to those of the laminin αB gene epi-1

C. elegans contains single laminin β and γ chains and two α chains, LAM-3/laminin-αA and EPI-1/laminin-αB (Huang et al., 2003). Both laminin-α chains are distributed broadly in BMs, but EPI-1 uniquely localizes to the gonad BM. Gonad epithelialization fails in *epi-1* mutants (Huang et al., 2003), resulting in gonad rupture like that seen in *dgn-1(0)* (Fig. 5F). The penetrance of the gonad defect varies between *epi-1* alleles, but is 100% in the putative null allele *rh199* (Table 1). SGP mispositioning is seen in newly hatched *rh199* animals, although at a higher penetrance than in *dgn-1* mutants (Fig. 5H). The similarity of gonad phenotypes suggests that DGN-1 may be a crucial receptor for EPI-1 in the gonad primordium.

epi-1 mutants show other morphological defects reminiscent of *dgn-1* phenotypes, although they often are more severe (Table 1). On average, three to four excretory cell arms are missing in *rh199* animals, compared with one to two in *cg121*, and remaining arms are short, and exhibit aberrant morphology and guidance. *epi-1*

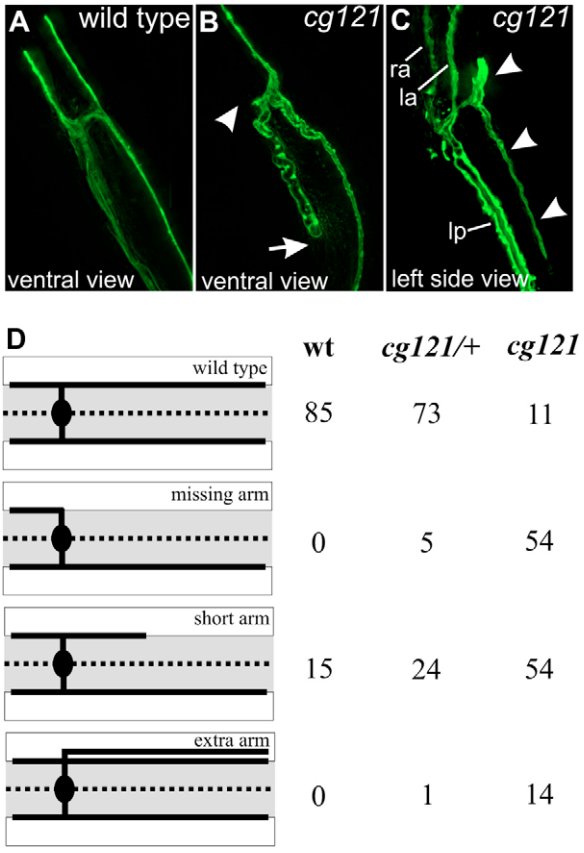

Fig. 8. Defects in excretory cell processes in *dgn-1* mutants. (**A**) H-shaped excretory cell of a wild-type animal. (**B**) Homozygous *cg121* null mutants frequently have short (arrow) or missing (arrowhead) excretory cell arms. (**C**) Null mutants also show arm duplications (arrowheads) but at a lower frequency (ra/la, right/left anterior; lp, left posterior arms). (**D**) Percentage of wild type, *cg121* homozygotes or *cg121/+* heterozygotes with the indicated defect in at least one excretory cell arm. Multiple defects can be present in a single animal, so values do not add to 100%.

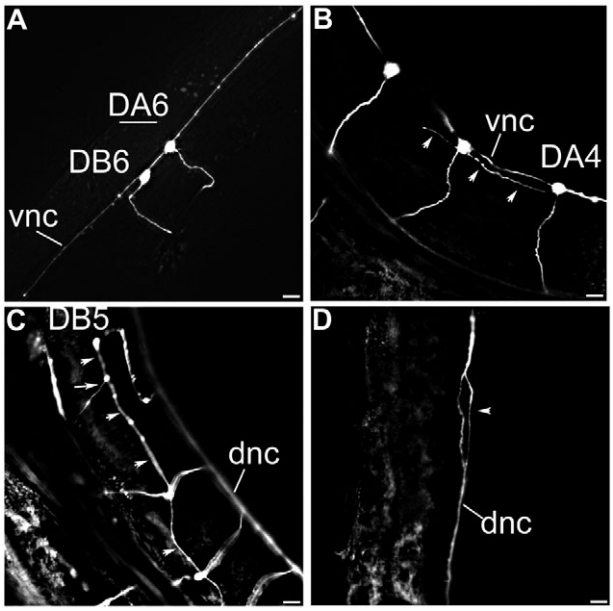

Fig. 9. Neural guidance defects in *dgn-1* mutants. Homozygous and heterozygous *dgn-1* mutants have axon guidance, branching and fasciculation defects in the DA/DB motoneurons (marker: *evIs82[unc-129::GFP]*). (**A**) Approximately 31% of *dgn-1(cg121)* homozygotes have side-switching defects in commissural DA/DB axons, which migrate from the ventral nerve cord (vnc) to the dorsal nerve cord (dnc). Heterozygotes show side-switching at a lower frequency. In this *cg121*/+ heterozygote, the DA6 commissure is abnormally extending on the right side, while the neighboring DB6 commissure is correctly extending on the right. (**B-D**) A variety of other, low penetrance defects are also seen in *dgn-1* mutants. (B) Extra process arising from the neural cell body (arrowheads). (C) Abnormal axon branching (arrow) and aberrant anterior/posterior migration of processes (arrowheads). (D) Defasciculation (arrowhead) of axons in the dorsal nerve cord. Anterior is down in each image. Scale bar: 10 μm.

mutants also show Pvl defects comparable to *dgn-1* mutants. These results are consistent with DGN-1 mediating some EPI-1 function in the development of the excretory cell and vulval epithelium.

Mutants of DAPC components do not show dgn-1 mutant morphological defects

DG function in vertebrate muscle is mediated by the DAPC complex containing dystrophin and associated proteins (Winder, 2001). We examined *C. elegans* DAPC mutants of *dys-1* dystrophin, *dyb-1* dystrobrevin and *stn-1* syntrophin for morphological phenotypes similar to those of *dgn-1*. None of these putative functional null mutants show the morphological defects prevalent in *dgn-1(0)* (Fig. 5, Table 1), indicating that the morphological functions of DGN-1 are largely independent of DAPC function.

Distinct behavioral phenotypes of dgn-1 and dystrophin complex mutants

C. elegans DAPC mutants display a head muscle hypercontraction phenotype (Fig. 10A) due to excessive acetylcholine neurotransmission (Kim et al., 2004). Hypercontraction is apparent in 100% of *dys-1*, *dyb-1* or *stn-1* mutants and occurs in at least 97% of movement cycles in each mutant (*n*=20 L4 animals, each observed for 50 movement cycles), but is not seen in *dgn-1* mutants. Double mutants of *dgn-1* with *dys-1*, *dyb-1* or *stn-1* show hypercontraction as in the DAPC single mutants (Fig. 10B), indicating that *dgn-1(cg121)* does not epistatically suppress this phenotype.

Table 1. Comparison of *dgn-1* mutant morphological phenotypes to *epi-1*/laminin αB and DAPC component mutants

	Gonad rupture	Protruding vulva	Excretory cell defects*	Motoneuron axon misguidance†
dgn-1(cg121)	100	45.1	89.0	31.0
epi-1(rh199)	100	78.4	100	nd‡
epi-1(rh92)	65.9	68.9	nd	nd‡
epi-1(rh27)	56.0	38.7	100	nd‡
dys-1(cx18)	0	0	0	5.6
dyb-1(cx36)	0	3	2.6	3.5
stn-1(ok292)	0	0	0	3.7

Percentage of animals (*n*=60-200) showing gonad rupture, vulval protrusion, excretory cell morphology or DA/DB motoneuron axon misguidance is indicated.
*Scored as percent animals with missing, short or duplicated excretory cell arms.
†Scored as left/right misdirection of DA/DB commissures, visualized by *evIs82*. DA/DB misguidance with *evIs82* in a wild-type background is 4.3%.
‡Specific DA/DB misguidance was not quantified because of the extensive neural disorganization in *epi-1* mutants.
nd, not determined.

DAPC mutants also display hyperactivity on agar plates (Bessou et al., 1998; Gieseler et al., 2001; Grisoni et al., 2003), generating 37%-57% more body bends per minute than wild type (Fig. 10C). The *dgn-1(cg121)* mutant shows comparable hyperactivity in plate locomotion (Fig. 10C). Both DAPC and *dgn-1* mutants also show a 9%-29% increase in thrashing rate when suspended in liquid (Fig. 10C). Double mutants show activity levels comparable to or slightly lower than wild type (Fig. 10C). Cross-suppression of hyperactivity in double mutants is inconsistent with DGN-1 and DAPC acting in a common functional pathway, and indicates that hyperactivity of *dgn-1* and DAPC mutants involves genetically distinct mechanisms.

dgn-1 homozygotes (Fig. 10D) show a 27% increase in defecation cycle time (Avery and Thomas, 1997) when compared with wild type (61±6 seconds versus 48±3 seconds). *dys-1* mutants display essentially normal periodicity (51±4 seconds), and *dys-1;dgn-1* double mutants have periodicity comparable with *dgn-1* single mutants (66±4 seconds). Together, these phenotypic comparisons indicate that DGN-1 and the DAPC complex of *C. elegans* function in different processes and act independently of one another.

DISCUSSION

A family of DG-like genes in metazoans

The DG-like genes in *C. elegans* and related nematodes define a family of proteins sharing a core region corresponding to the C terminus of vertebrate α-DG and the extracellular region of β-DG. The vertebrate DG core contains the site of post-translational α/β cleavage and sites within α and β subunits mediating their association (Sciandra et al., 2001). DGN-1 and *Drosophila* DG (Deng et al., 2003) are not processed into separate α and β subunits, although interaction of the corresponding regions may occur. Interestingly, a mutant DG in which α/β cleavage is disrupted dominantly produces altered DG glycosylation and muscular dystrophy in mice (Jayasinha et al., 2003), suggesting a regulatory role for vertebrate α/β cleavage. The core region also contains conserved potential N-linked glycosylation sites important in intracellular trafficking of DG (Holt et al., 2000). The core domain may mediate conserved interactions with as yet unidentified extracellular or transmembrane factors.

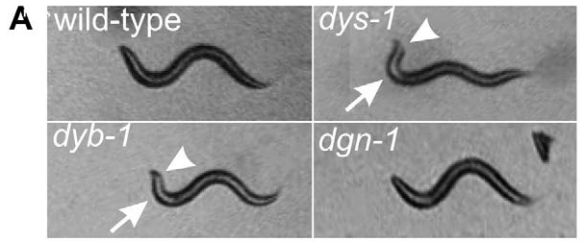

B

	head hypercontraction?
wild type	-
dgn-1	-
dys-1	+
dyb-1	+
stn-1	+
dys-1;dgn-1	+
dyb-1;dgn-1	+
stn-1;dgn-1	+

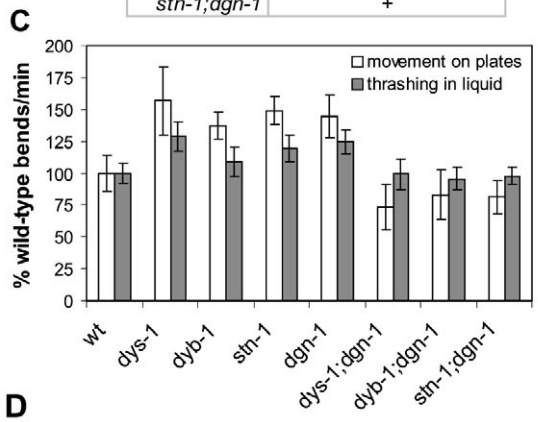

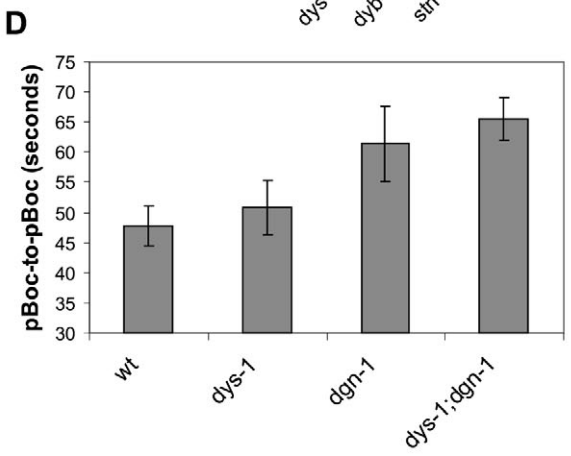

Fig. 10. *C. elegans* DAPC and *dgn-1* mutants have distinct behavioral phenotypes. (**A**) Hypercontraction of the head musculature (arrowhead, arrow) in DAPC component mutants *dys-1(cx18)* and *dyb-1(cx36)*, but not in *dgn-1(cg121)*, during movement on plates. (**B**) Double mutants of *dgn-1* and DAPC components show hypercontraction. (**C**) Activity (body bends per minute) during movement on agar plates or during thrashing in liquid. Measurements were normalized to wild-type (wt) values (plate movement, 100%=30.1 bends/minute; thrashing, 100%=167.9 bends/minute). Both *dgn-1(cg121)* and DAPC mutants are hyperactive, but double mutants show wild-type or lower rates. (**D**) Prolongation of the Pboc-to-Pboc defecation cycle time in the *dgn-1(cg121)* and in *dgn-1;dys-1* double mutants, but not in the *dys-1(cx18)* mutant itself. In C and D, the mean and standard deviation (error bars) of 8-10 animals is reported.

Distinct N-terminal and C-terminal domains distinguish the members of the DG family. DGN-1, *Drosophila* and vertebrate DGs comprise an orthologous subfamily with conserved roles as BM receptors (Deng et al., 2003; Parsons et al., 2002; Winder, 2001) (this work). Multiple *Caenorhabditis* species contain additional species-specific, more divergent, DG-like genes whose roles remain to be elucidated. *C. elegans dgn-2* and *dgn-3* are expressed in a few neural and epithelial cells, and deletion mutations cause no overt phenotypes (J.M.K., unpublished). It is possible that the N-terminal and C-terminal domains of these divergent DG-like proteins mediate distinct transmembrane linkages between specific extracellular ligands and intracellular effectors.

DGN-1 is not generally required for BM assembly but is a likely mediator of laminin function in early gonad epithelium

BMs form and most are maintained in *dgn-1(0)* mutants, although the gonad BM is not maintained in the absence of DGN-1. Similarly, vertebrate DG is not generally essential for BM assembly (Li et al., 2002) but may play an important role in some contexts (Henry and Campbell, 1998). Mouse embryos lacking DG do not form Reichert's membrane, but form the epiblast BM in the embryo proper (Williamson et al., 1997). In a brain-specific DG knockout, the pial BM forms but contains focal discontinuities (Moore et al., 2002). Thus, in both nematodes and vertebrates the DG ortholog has roles in the maintenance of specific BMs but is not required for all BM assembly.

The similar gonad primordium defects in *epi-1* and *dgn-1* mutants suggest that DGN-1 is a likely mediator of EPI-1 function in the early gonad. The single *C. elegans* β integrin PAT-3 is another potential laminin receptor, but dominant interference of PAT-3 function does not appear to produce the same early gonad phenotype (Lee et al., 2001). DGN-1 is not required for the initial localization of laminin to the surface of the primordium, indicating that other factors mediate laminin recruitment. EPI-1 functioning through DGN-1 appears to be essential for promoting the epithelial function of the SGPs, although the nature of this nascent epithelium is unclear. Somatic cells of the early gonad do not display junctional complexes indicative of mature polarized epithelia and do not express identified junctional components (Miskowski et al., 2001). A BM signal through DGN-1 may play a role in the apicobasal polarization of somatic gonad cells in the early gonad, before a mature epithelium has differentiated.

Early gonad disruption in *dgn-1* and *epi-1* mutants results in the escape of germ cell precursors into the body cavity. The gonad BM may be important structurally to maintain ensheathment by the somatic gonad cells, but it is also possible that an unidentified DGN-1-mediated signal from the gonad BM promotes germ-soma interaction. DGN-1 function is not required for the adhesion of somatic gonad cells with one another. Somatic gonad cells cluster together in *dgn-1(0)* L2 stage animals, and differentiated spermathecal and uterine cells displaying AJM-1-containing cell junctions and lumen formation are found in L4 stage animals.

A role for DGN-1 in the migration of cells and specialized cell processes

Migrations of axons and the tubular arms of the excretory cell involve the extension of cell processes between the hypodermis and its BM (Wood, 1988), and several cell adhesion and cytoskeletal factors, including laminin, are involved in their guidance (Buechner, 2002). The excretory cell and axonal guidance

phenotypes of *dgn-1* and *epi-1* mutants suggest that DGN-1 partially mediates laminin function in guiding cell processes along the hypodermal BM.

Heterozygous *dgn-1(0)*/+ animals show defects in excretory cell and axon migration, as well as in DTC guidance along BMs. DGN-1 may have an essential role in DTC migration that cannot be assessed directly because of the gonad disruption in *dgn-1(0)* homozygotes. The defects in excretory cell, DTC and axon migration in *cg121*/+ heterozygotes must represent haploinsufficiency, in which the reduced DGN-1 levels in heterozygotes are insufficient for normal function. DGN-1 overexpression from extrachromosomal arrays can also cause *dgn-1(0)*-like defects in wild-type animals, particularly in excretory cell morphology (R.P.J., unpublished). The appearance of similar phenotypes from increased or decreased expression suggests that DGN-1 activity may be required dynamically and/or in precise stoichiometry relative to other components for normal function.

Conserved epithelial and neural roles for DG

DGN-1 functions in a variety of epithelia and neurons but is not expressed in muscle. Vertebrate DG also functions in the nervous system (Moore et al., 2002; Saito et al., 2003) and in at least some types of epithelia (Durbeej et al., 1995; Durbeej et al., 2001), as well as in muscle. In *Drosophila*, DG is important in the polarization of follicular epithelia and oocytes (Deng et al., 2003), although it is expressed and may have additional roles in muscle and neural tissue (Dekkers et al., 2004). These findings suggest that either the DGN-1/DG subfamily originated as an ECM receptor in epithelial/neural tissue and that muscle function was acquired later, or that an original muscle role for DG was not retained in nematodes. Notably, each sarcomere in nematode muscle is anchored to the underlying BM via integrin-containing dense bodies (Moerman and Fire, 1997), and these numerous attachments may preclude the need for further sarcolemmal stabilization by DGN-1.

Divergence of DGN-1 and DAPC complex functions in *C. elegans*

DGN-1 functions in epithelia and neurons do not depend on the conserved DAPC complex, which is consistent with the poor conservation of the dystrophin-binding site in the DGN-1 cytoplasmic domain. The major site of DAPC function is in muscle, where it regulates contraction intensity via the acetylcholine transporter SNF-6 (Bessou et al., 1998; Gieseler et al., 2001; Grisoni et al., 2003; Kim et al., 2004). It is unclear whether the hyperactivity of DAPC mutants (Bessou et al., 1998; Gieseler et al., 2001; Grisoni et al., 2003) is also due to altered cholinergic stimulation. *dgn-1* mutants show similar hyperactivity that is genetically distinct from that of the DAPC mutants and may reflect neuronal DGN-1 function.

The divergence of DGN-1 and DAPC complex function in *C. elegans* has intriguing implications for the normal and pathological roles of their vertebrate homologs. The progressive muscle degeneration in *C. elegans* DAPC and *snf-6* mutants is reminiscent of vertebrate muscular dystrophy (Bessou et al., 1998; Gieseler et al., 2001; Grisoni et al., 2003; Kim et al., 2004; Cohn and Campbell, 2000) and may reflect a conserved muscle function of the DAPC that is separable from its interaction with DG. Conversely, evidence from vertebrate systems suggests that non-muscle DG may have roles not requiring DAPC function. Several studies indicate that vertebrate DG has important functions in the early embryo and in non-muscle tissues that do not appear to depend on DAPC or sarcoglycan complex function, but do depend on the ECM ligand-binding activity of α-DG (Durbeej et al., 1995; Durbeej et al., 2001; Michele et al., 2002; Moore et al., 2002; Rafael et al., 1999; Imamura et al., 2000; Saito et al., 2003; Williamson et al., 1997). Thus, non-muscle DG probably mediates important ECM interactions that are wholly or partly independent of DAPC function, suggesting that other intracellular factors transduce DG function in these contexts. The DAPC-independent roles of DGN-1 in *C. elegans* may thus help to elucidate conserved non-muscle roles of DG as a BM receptor and to identify novel downstream partners of DG.

We thank Y. Kohara for providing *dgn-1* cDNA clones. Some strains used in this work were provided by the *C. elegans* Genetics Center, which is funded by the NIH National Center for Research Resources (NCRR). This work was supported by NIH grant HD27211.

References

Altschul, S. F., Gish, W., Miller, W., Myers, E. W. and Lipman, D. J. (1990). Basic local alignment search tool. *J. Mol. Biol.* **215**, 403-410.
Avery, L. and Thomas, J. H. (1997). Feeding and defecation. In *C. elegans II* (ed. D. L. Riddle, T. Blumenthal, B. J. Meyer and J. R. Priess), pp. 679-716. New York: Cold Spring Harbor Laboratory Press.
Barstead, R. J. (1999). Reverse genetics. In *C. elegans: A Practical Approach* (ed. I. A. Hope), pp. 97-118. Oxford: Oxford University Press.
Bessou, C., Giugia, J. B., Franks, C. J., Holden-Dye, L. and Segalat, L. (1998). Mutations in the *Caenorhabditis elegans* dystrophin-like gene *dys-1* lead to hyperactivity and suggest a link with cholinergic transmission. *Neurogenetics* **2**, 61-72.
Bozic, D., Sciandra, F., Lamba, D. and Brancaccio, A. (2004). The structure of the N-terminal region of murine skeletal muscle alpha-DG discloses a modular architecture. *J. Biol. Chem.* **279**, 44812-44816.
Brancaccio, A., Jeno, P. and Engel, J. (1998). A single disulfide bridge (Cys182-Cys264) is crucial for alpha-DG N-terminal domain stability. *Ann. N. Y. Acad. Sci.* **857**, 228-231.
Brenner, S. (1974). The genetics of *Caenorhabditis elegans*. *Genetics* **77**, 71-94.
Buechner, M. (2002). Tubes and the single C. elegans excretory cell. *Trends Cell Biol*. **12**, 479-484.
Cohn, R. D. and Campbell, K. P. (2000). Molecular basis of muscular dystrophies. *Muscle Nerve* **23**, 1456-1471.
Cohn, R., Henry, M., Michele, D., Barresi, R., Saito, F., Moore, S., Flanagan, J., Skwarchuk, M., Robbins, M., Mendell, J. et al. (2002). Disruption of dag1 in differentiated skeletal muscle reveals a role for DG in muscle regeneration. *Cell* **110**, 639.
Cote, P. D., Moukhles, H., Lindenbaum, M. and Carbonetto, S. (1999). Chimaeric mice deficient in DGs develop muscular dystrophy and have disrupted myoneural synapses. *Nat. Genet*. **23**, 338-342.
Dekkers, L. C., van der Plas, M. C., van Loenen, P. B., den Dunnen, J. T., van Ommen, G. J., Fradkin, L. G. and Noordermeer, J. N. (2004). Embryonic expression patterns of the Drosophila dystrophin-associated glycoprotein complex orthologs. *Gene Expr. Patterns* **4**, 153-159.
Deng, W.-M., Schneider, M., Frock, R., Castillejo-Lopez, C., Gaman, E. A., Baumgartner, S. and Ruohola-Baker, H. (2003). DG is required for polarizing the epithelial cells and the oocyte in Drosophila. *Development* **130**, 173-184.
Deyst, K. A., Bowe, M. A., Leszyk, J. D. and Fallon, J. R. (1995). The alpha-DG-beta-DG complex – Membrane organization and relationship to an agrin receptor. *J. Biol. Chem.* **270**, 25956-25959.
Durbeej, M., Larsson, E., Ibraghimov-Beskrovnaya, O., Roberds, S. L., Campbell, K. P. and Ekblom, P. (1995). Non-muscle alpha-DG is involved in epithelial development. *J. Cell Biol.* **130**, 79-91.
Durbeej, M., Talts, J. F., Henry, M. D., Yurchenco, P. D., Campbell, K. P. and Ekblom, P. (2001). DG binding to laminin alpha1LG4 module influences epithelial morphogenesis of salivary gland and lung in vitro. *Differentiation* **69**, 121-134.
Gieseler, K., Mariol, M.-C., Bessou, C., Migaud, M., Franks, C. J., Holden-Dye, L. and Ségalat, L. (2001). Molecular, genetic and physiological characterization of dystrobrevin-like (dyb-1) mutants of Caenorhabditis elegans. *J. Mol. Biol*. **307**, 107-117.
Greenwald, I. (1997). Development of the vulva. In *C. elegans II* (ed. D. L. Riddle, T. Blumenthal, B. J. Meyer and J. R. Priess), pp. 519-541. New York: Cold Spring Harbor Laboratory Press.
Grisoni, K., Martin, E., Gieseler, K., Mariol, M. C. and Segalat, L. (2002). Genetic evidence for a dystrophin-glycoprotein complex (DGC) in Caenorhabditis elegans. *Gene* **294**, 77-86.
Grisoni, K., Gieseler, K., Mariol, M. C., Martin, E., Carre-Pierrat, M., Moulder, G., Barstead, R. and Segalat, L. (2003). The stn-1 syntrophin gene of C.elegans is functionally related to dystrophin and dystrobrevin. *J. Mol. Biol*. **332**, 1037-1046.
Henry, M. D. and Campbell, K. P. (1998). A role for DG in BM assembly. *Cell* **95**, 859-870.

Hohenester, E., Tisi, D., Talts, J. F. and Timpl, R. (1999). The crystal structure of a laminin G-like module reveals the molecular basis of alpha-DG binding to laminins, perlecan, and agrin. *Mol. Cell*. **4**, 783-792.
Holt, K. H., Crosbie, R. H., Venzke, D. P. and Campbell, K. P. (2000). Biosynthesis of DG: processing of a precursor propeptide. *FEBS Lett*. **468**, 79-83.
Huang, C.-C., Hall, D. H., Hedgecock, E. M., Kao, G., Karantza, V., Vogel, B. E., Hutter, H., Chisholm, A. D., Yurchenco, P. D. and Wadsworth, W. G. (2003). Laminin alpha subunits and their role in C. elegans development. *Development* **130**, 3343-3358.
Huang, X., Poy, F., Zhang, R., Joachimiak, A., Sudol, M. and Eck, M. J. (2000). Structure of a WW domain containing fragment of dystrophin in complex with beta-DG. *Nat. Struct. Biol*. **7**, 634-638.
Ibraghimov-Beskrovnaya, O., Ervasti, J. M., Leveille, C. J., Slaughter, C. A., Sernett, S. W. and Campbell, K. P. (1992). Primary structure of dystrophin-associated glycoproteins linking dystrophin to the extracellular matrix. *Nature* **355**, 696-702.
Imamura, M., Araishi, K., Noguchi, S. and Ozawa, E. (2000). A sarcoglycan-DG complex anchors Dp116 and utrophin in the peripheral nervous system. *Hum. Mol. Genet*. **9**, 3091-3100.
Inoue, T., Sherwood, D. R., Aspock, G., Butler, J. A., Gupta, B. P., Kirouac, M., Wang, M., Lee, P.-Y., Kramer, J. M. and Hope, I. (2002). Gene expression markers for Caenorhabditis elegans vulval cells. *Gene Expr. Patterns* **2**, 235-241.
Jayasinha, V., Nguyen, H. H., Xia, B., Kammesheidt, A., Hoyte, K. and Martin, P. T. (2003). Inhibition of DG cleavage causes muscular dystrophy in transgenic mice. *Neuromuscul. Disord*. **13**, 365-375.
Kang, S. H. and Kramer, J. M. (2000). Nidogen is nonessential and not required for normal type IV collagen localization in *Caenorhabditis elegans*. *Mol. Biol Cell*. **11**, 3911-3923.
Kim, H., Rogers, M. J., Richmond, J. E. and McIntire, S. L. (2004). SNF-6 is an acetylcholine transporter interacting with the dystrophin complex in *Caenorhabditis elegans*. *Nature* **430**, 891-896.
Lee, M., Cram, E. J., Shen, B. and Schwarzbauer, J. E. (2001). Roles for beta pat-3 integrins in development and function of *Caenorhabditis elegans* muscles and gonads. *J. Biol. Chem*. **276**, 36404-36410.
Li, S., Harrison, D., Carbonetto, S., Fässler, R., Smyth, N., Edgar, D. and Yurchenco, P. D. (2002). Matrix assembly, regulation, and survival functions of laminin and its receptors in embryonic stem cell differentiation. *J. Cell Biol*. **157**, 1279-1290.
Mello, C. C., Kramer, J. M., Stinchcomb, D. and Ambros, V. (1991). Efficient gene transfer in *C. elegans*: extrachromosomal maintenance and integration of transforming sequences. *EMBO J*. **10**, 3959-3970.
Michele, D. E. and Campbell, K. P. (2003). Dystrophin-glycoprotein complex: post-translational processing and DG function. *J. Biol. Chem*. **278**, 15457-15460.
Michele, D. E., Barresi, R., Kanagawa, M., Saito, F., Cohn, R. D., Satz, J. S., Dollar, J., Nishino, I., Kelley, R. I., Somer, H. et al. (2002). Post-translational disruption of DG-ligand interactions in congenital muscular dystrophies. *Nature* **418**, 417-422.
Miskowski, J., Li, Y. and Kimble, J. (2001). The sys-1 gene and sexual dimorphism during gonadogenesis in Caenorhabditis elegans. *Dev. Biol.* **230**, 61-73.
Moerman, D. G. and Fire, A. (1997). Muscle: structure, function, and development. In *C. elegans II* (ed. D. L. Riddle, T. Blumenthal, B. J. Meyer and J. R. Priess), pp. 417-470. New York: Cold Spring Harbor Laboratory Press.
Moore, S. A., Saito, F., Chen, J., Michele, D. E., Henry, M. D., Messing, A., Cohn, R. D., Ross-Barta, S. E., Westra, S., Williamson, R. A. et al. (2002). Deletion of brain DG recapitulates aspects of congenital muscular dystrophy. *Nature* **418**, 422-425.
Muschler, J., Levy, D., Boudreau, R., Henry, M., Campbell, K. and Bissell, M. J. (2002). A role for DG in epithelial polarization: loss of function in breast tumor cells. *Cancer Res*. **62**, 7102-7109.
Parsons, M. J., Campos, I., Hirst, E. M. A. and Stemple, D. L. (2002). Removal of DG causes severe muscular dystrophy in zebrafish embryos. *Development* **129**, 3505-3512.
Rafael, J. A., Trickett, J. I., Potter, A. C. and Davies, K. E. (1999). Dystrophin and utrophin do not play crucial roles in nonmuscle tissues in mice. *Muscle Nerve* **22**, 517-519.
Saito, F., Moore, S. A., Barresi, R., Henry, M. D., Messing, A., Ross-Barta, S. E., Cohn, R. D., Williamson, R. A., Sluka, K. A., Sherman, D. L. et al. (2003). Unique role of DG in peripheral nerve myelination, nodal structure, and sodium channel stabilization. *Neuron* **38**, 747-758.
Sciandra, F., Schneider, M., Giardina, B., Baumgartner, S., Petrucci, T. C. and Brancaccio, A. (2001). Identification of the beta-DG binding epitope within the C-terminal region of alpha-DG. *Eur. J. Biochem*. **268**, 4590-4597.
Su, M.-W., Merz, D. C., Killeen, M. T., Zhou, Y., Zheng, H., Kramer, J. M., Hedgecock, E. M. and Culotti, J. G. (2000). Regulation of the UNC-5 netrin receptor initiates the first reorientation of migrating distal tip cells in Caenorhabditis elegans. *Development* **127**, 585-594.
Thompson, J. D., Higgins, D. G. and Gibson, T. J. (1994). CLUSTAL W: improving the sensitivity of progressive multiple sequence alignment through sequence weighting, position-specific gap penalties and weight matrix choice. *Nucleic Acids Res.* **22**, 4673-4680.
Williamson, R. A., Henry, M. D., Daniels, K. J., Hrstka, R. F., Lee, J. C., Sunada, Y., Ibraghimov-Beskrovnaya, O. and Campbell, K. P. (1997). DG is essential for early embryonic development: disruption of Reichert's membrane in Dag1-null mice. *Hum. Mol. Genet*. **6**, 831-841.
Winder, S. J. (2001). The complexities of DG. *Trends Biochem. Sci*. **26**, 118-124.
Wood, W. B. (1988). *The Nematode Caenorhabditis elegans* (ed. W. B. Wood). New York: Cold Spring Harbor Laboratory Press.